

Melting Behavior and Crystallization Kinetics of Starch and Poly(lactic acid) Composites

Tianyi Ke, Xuzhi Sun

Department of Grain Science and Industry, Kansas State University, Manhattan, Kansas 66506

Received 1 April 2002; accepted 9 September 2002

ABSTRACT: Differential scanning calorimetry was used to characterize the melting behavior and isothermal crystallization kinetics of pure poly(lactic acid) (PLA) and blends of PLA with various corn starch contents at varying isothermal crystallization temperatures (90–125°C). The experimental data were evaluated using the well-known Avrami kinetic model. The Avrami exponent, constant, half-time of crystallization, and degree of crystallinity were obtained. Talc, a nucleating agent, was also blended with PLA at 1% by volume (v/v) as a comparison. Starch effectively increased

the crystallization rate of PLA, even at a 1% content, but the effect was less than that of talc. The crystallization rate of PLA increased slightly as the starch content in the blend was increased from 1 to 40%. An additional crystallization of PLA was observed, and it affected the melting point and degree of crystallinity of PLA. © 2003 Wiley Periodicals, Inc. *J Appl Polym Sci* 89: 1203–1210, 2003

Key words: poly(lactic acid); starch; blends; isothermal crystallization kinetics

INTRODUCTION

Poly(lactic acid) (PLA) is a disposable and biodegradable plastic that is being developed as a substitute for petroleum thermoplastics. Because it is expensive, PLA has been blended with starch to reduce production costs. Previous studies showed that starch/PLA blends are affected by several variables, including the starch ratio, starch moisture content, blend heat treatment, plasticizers, and coupling agents.^{1–3} PLA plays the key role in PLA/starch composites, dominating the mechanical and biodegradation properties of the blends. The microstructure of PLA, which is formed during thermal processing, has a significant effect on its ultimate product quality. Researchers have studied the crystallization behavior,^{4–7} especially the crystallization kinetics,^{8,9} of PLA; the isothermal melting mechanism¹⁰ of PLA; the effects of undercooling and the molecular weight of PLA on its morphology and crystal growth;¹¹ the effects of annealing on the thermal properties, morphology, and mechanical properties of PLA films;¹² and the effects of thermal treatment on compression-molded PLA at different molecular weights.¹³ However, there is little information about how the starch content might influence the PLA crystallization kinetics.

The objective of the present study was to characterize the crystallization behavior of PLA in PLA/starch composites using differential scanning calorimetry (DSC) at various controlled crystallization temperatures. This information would be useful to better understand starch/PLA composites and their manufacturing.

EXPERIMENTAL

Materials and sample preparation

Industrial corn starch (Silver Medal Pearl-1100) was purchased from Cargill, Inc. (Minneapolis, MN). The PLA was obtained from Shimadzu, Inc. It had a molecular weight of about 120,000 Da and was polymerized mainly from L-lactic acid.

The corn starch was dried in an air oven at 130°C for about 2 h. The PLA was ground into small particles (about 2 mm). Dried corn starch and ground PLA

TABLE I
Sample Codes of PLA and Its Blends with Starch and Talc

Code	Filler (%)	PLA (%)
Pla	0	100
	Corn starch	
CnPla1-99	1	99
CnPla4-96	4	96
CnPla10-90	10	90
CnPla20-80	20	80
CnPla40-60	40	60
	Talc	
TalcPla1-99	1	99

This article is Kansas Agricultural Experiment Station contribution 02-365-J.

Correspondence to: X. S. Sun (xss@ksu.edu).

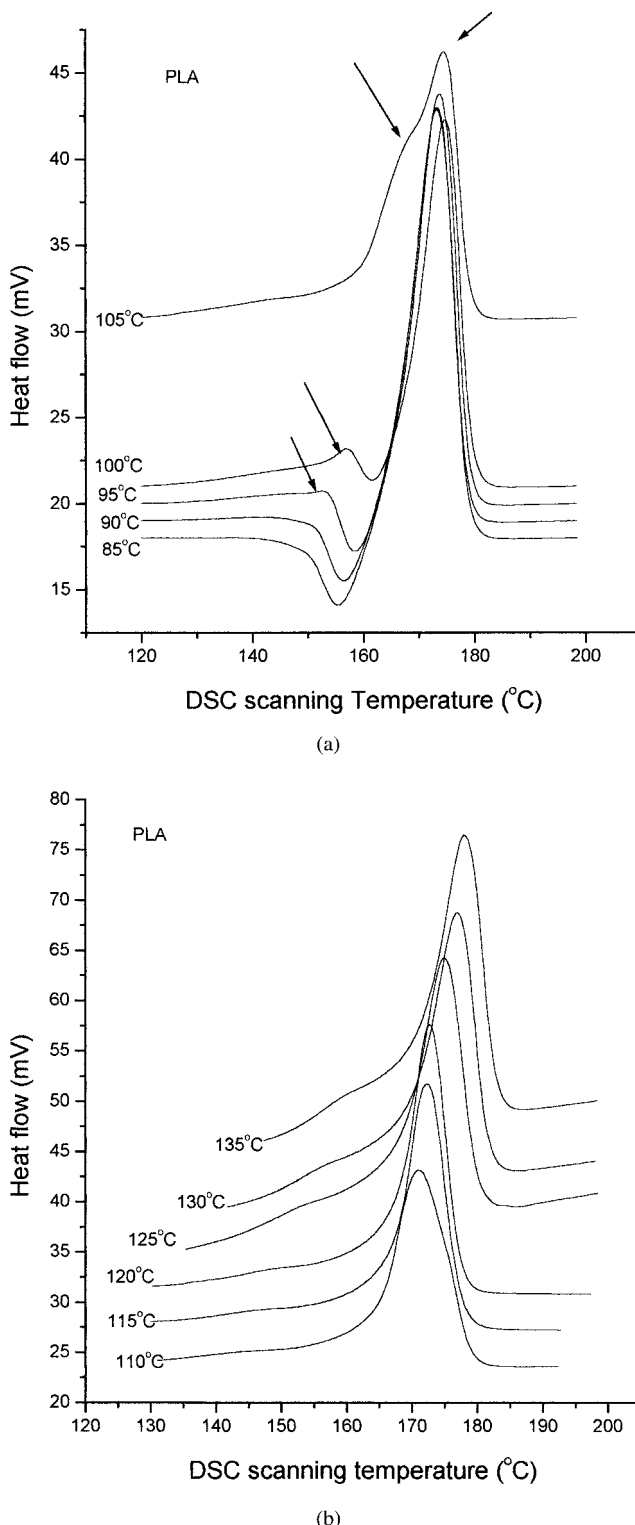


Figure 1 DSC melting thermograms of pure PLA after isothermal crystallization (T_c) at (A) 85–105 and (B) 110–135°C.

were premixed using a stand mixer (Ultra Power Kitchen Aid, St. Joseph, MI) at starch/PLA weight ratios (w/w) of 1:99, 4:96, 7:93, 10:90, 20:80, and 40:60 at ambient conditions. The mixture was stored in a

polyethylene Ziplock® plastic bag for about 1 h. Then it was blended in a lab-scale corotating conical twin-screw extruder (TW-100, Haake, Paramus, NJ), which has a screw diameter of 19.1 mm, a length to diameter ratio of 25:1, and constant pitch and constant flight depth.

Each mixture was loaded into a feeding funnel by hand. It was extruded through a rod die with an 8-mm diameter aperture at a temperature profiles of 120 (zone 1, near the feed inlet), 185 (zone 2), 185 (zone 3), and 185°C (at the die). The screw speed was fixed at 100 rpm. The output rate was about 15 g/min. The extruded rods were cut into short cylinders about 10 mm in length and then were ground into small particles of about 2 mm using a mill (model 4 laboratory mill, Thomas-Wiley Company, Philadelphia, PA). Samples were stored in a dessicator at ambient temperature until analysis.

Samples containing talc (1%), a nucleating agent, were made according to the same procedures described for forming starch and PLA blends.

Thermal analysis

Isothermal crystallization characterization was performed by using a Perkin-Elmer DSC 7 system (Norwalk, CT). The DSC 7 was calibrated using the melting temperature and enthalpy of indium, the standard material. The dried and ground blend samples were accurately weighed into an aluminum pan and hermetically sealed. The amount of PLA in the DSC samples was 15 mg. An empty pan was used as a reference. For crystallization characterization, a sample was heated from 25 to 200°C at 20°C/min and maintained at 200°C for 5 min. Subsequently, it was rapidly cooled (~80°C/min) to the isothermal evaluation temperature. Isothermal temperatures ranged from 85 to 135°C at 5°C intervals and the sample was held at each isothermal temperature for 10–15 min, allowing complete crystallization. To observe the melting behavior,

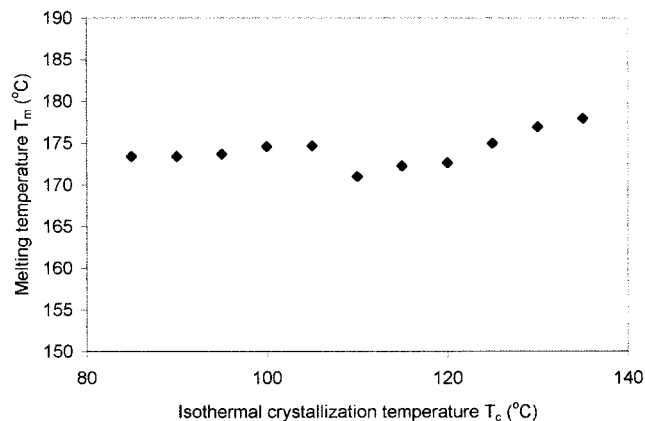


Figure 2 The melting peak temperature of pure PLA as affected by isothermal crystallization temperatures (T_c).

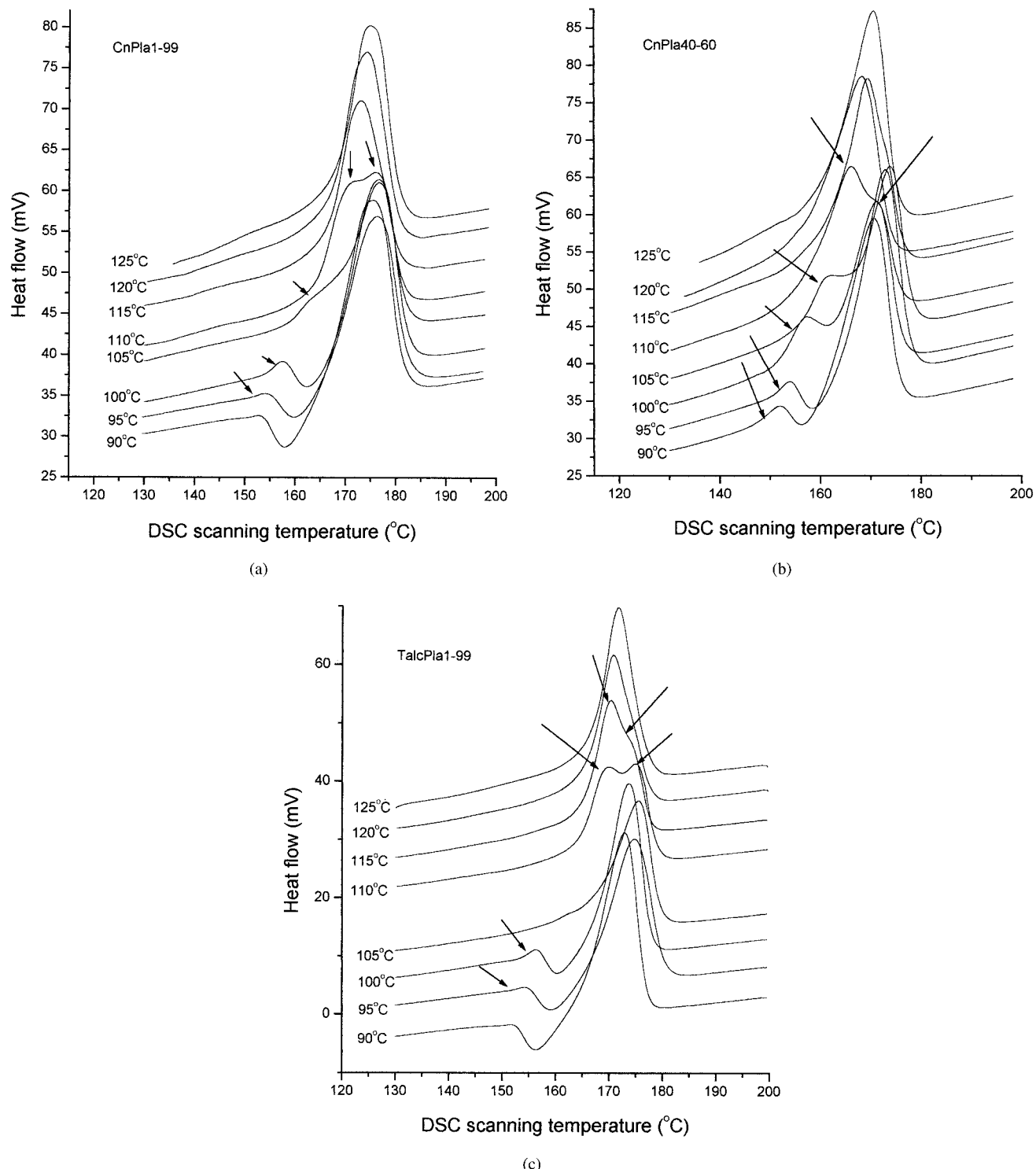


Figure 3 DSC melting thermograms of PLA/starch blends and PLA/talc blends after isothermal crystallization at various temperatures (T_c). The ratio of (A) starch/PLA = 1:99, (B) starch/PLA = 4:96, and (C) talc/PLA = 1:99.

the isothermally crystallized samples were reheated to 200°C at a rate of 20°C/min. The melting temperature that was observed was taken as the maximum of the endothermic transition. Sample codes are listed in Table I.

Theory of isothermal crystallization kinetics

The Avrami¹⁴ equation below is widely used to describe the isothermal crystallization processes in polymers:

$$X(t) = X_\infty [1 - \exp(-Kt^n)] \quad (1)$$

TABLE II
Values of Fusion Enthalpy (H_f), Overall Kinetic Rate Constant (K_n), and Avrami Index (n) at Various Isothermal Crystallization Temperatures (T_c)

Sample codes	T_c (K)	H_f (J/g)	K_n (min ⁻¹)	n	n_{ave}	Sample codes	T_c (K)	H_f (J/g)	K_n (min ⁻¹)	n	n_{ave}
PLA	358	27.2	5.84×10^{-5}	2.64	2.19	CnPla4-96	378	39.7	1.19×10^{-1}	2.36	
	363	36.9	2.04×10^{-3}	2.06			383	38.4	1.45×10^{-1}	2.4	
	368	35.2	2.25×10^{-3}	2.42			388	45.5	2.07×10^{-2}	2.33	
	373	32.3	5.16×10^{-3}	2.23			393	51.3	1.15×10^{-2}	2.06	
	378	37.1	5.58×10^{-3}	2.09			398	56.3	6.85×10^{-3}	1.74	
	383	40.7	3.10×10^{-3}	2.1			363	32.5	1.80×10^{-2}	2.28	2.31
	388	44.0	2.47×10^{-3}	2.08			368	30.4	6.00×10^{-2}	2.29	
	393	51.0	1.08×10^{-3}	2.18			373	36.8	8.25×10^{-2}	2.36	
	398	50.8	2.63×10^{-3}	2.37			378	36.9	1.04×10^{-1}	2.3	
	403	54.8	1.04×10^{-4}	2.32			383	35.2	9.66×10^{-2}	2.41	
TacPla1-99	408	60.6	1.84×10^{-4}	2.06		CnPla10-90	388	45.5	2.04×10^{-2}	2.41	
	363	25.4	6.38×10^{-1}	2.05	1.78		393	49.5	4.07×10^{-3}	2.38	
	368	26.8	1.70	1.87			398	57.4	3.48×10^{-3}	2.03	
	373	30.3	2.80	1.69			363	46.1	5.39×10^{-2}	2.06	2.08
	378	27.9	4.16	1.73			368	34.2	6.85×10^{-2}	2.01	
	383	30.5	6.54	1.87			373	29.6	1.33×10^{-1}	2.15	
	388	24.8	8.98	1.72			378	40.9	2.15×10^{-1}	1.87	
	393	29.5	9.43	1.67			383	40.9	9.77×10^{-2}	2.02	
	398	26.7	9.78	1.67			388	47.2	5.31×10^{-2}	2.11	
	363	34.5	1.48×10^{-2}	2.36	2.27		393	48.8	1.76×10^{-2}	2.23	
CnPla1-99	368	35.9	3.83×10^{-2}	2.38		CnPla20-80	398	53.9	8.25×10^{-3}	2.21	
	373	37.2	1.07×10^{-1}	2.41			363	36.1	1.69×10^{-1}	1.67	1.90
	378	38.3	1.06×10^{-1}	2.31			368	31.3	1.25×10^{-1}	2.04	
	383	42.9	7.02×10^{-2}	2.33			373	41.7	4.24×10^{-1}	2.22	
	388	46.7	1.55×10^{-2}	2.36			378	40.4	7.10×10^{-1}	1.57	
	393	51.4	7.10×10^{-3}	2.11			383	47.2	1.88×10^{-1}	2.05	
	398	45.9	1.52×10^{-3}	2.03			388	49.0	9.85×10^{-2}	2	
	363	31.4	2.24×10^{-2}	2.33	2.25		393	58.4	4.13×10^{-2}	1.87	
	368	31.9	6.61×10^{-2}	2.36			398	55.4	2.13×10^{-2}	1.77	
	373	37.0	1.06×10^{-1}	2.39							

See Table I for sample codes.

where $X(t)$ is the volume crystallinity at time t ; X_∞ is the volume crystallinity after infinite time, which was estimated by using ΔH_∞ ; K is the overall kinetic rate constant; and n is the Avrami exponent, which depends on the nucleation and growth mechanism of the

crystal. The evolution of the crystallinity with time can be estimated by using the degrees of crystallization (α) as expressed by the ratio of enthalpy determined by DSC:

$$\alpha = X(t) / X_\infty = \Delta H_t / \Delta H_\infty$$

where

$$\Delta H_t = \int_0^t \left(\frac{dH}{dt} \right) dt$$

is the enthalpy at time t and

$$\Delta H_\infty = \int_0^\infty \left(\frac{dH}{dt} \right) dt$$

is the enthalpy at time t_∞ . (In this study, ΔH_∞ is the total area under the crystallization curve.)

It can be further expressed by

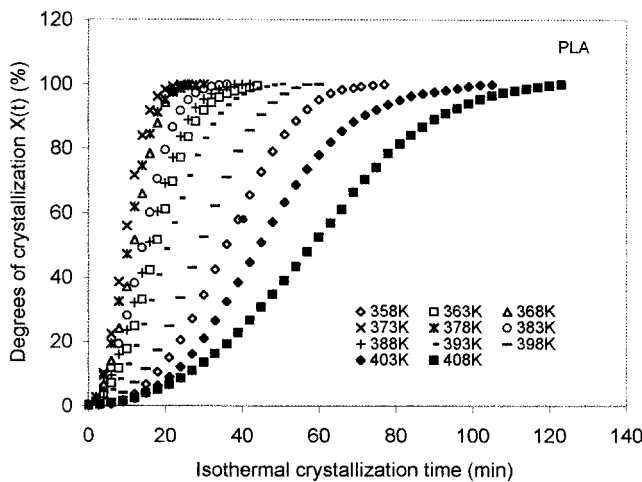


Figure 4 The relative degree of crystallization of PLA as a function of the isothermal crystallization time.

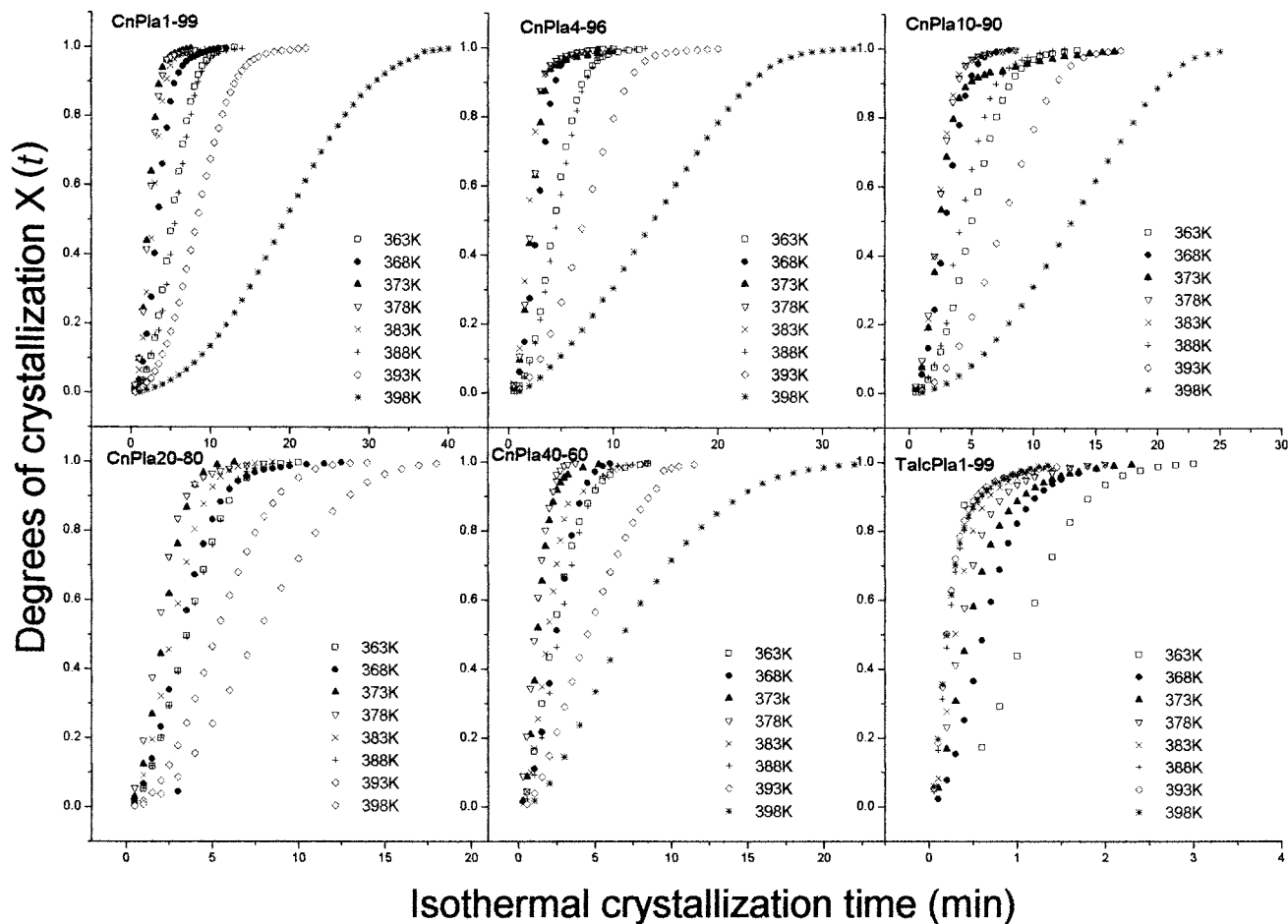


Figure 5 The relative degree of crystallization of PLA/starch blends and PLA/talc blends as a function of the isothermal crystallization time.

$$\alpha = \frac{\int_0^t \left(\frac{dH}{dt} \right) dt}{\int_0^\infty \left(\frac{dH}{dt} \right) dt}$$

where dH/dt is the respective heat flow and t_0 is the time at which the sample attains isothermal conditions, as indicated by a flat baseline after the initial spike in the thermal curve. In general, the Avrami equation is often converted to the traditional linear form:

$$\ln[-\ln(1 - \alpha)] = \ln K + n \ln(t) \quad (2)$$

In our experiment, the so-called Avrami plots $\ln[-\ln(1 - \alpha)]$ versus $\ln(t)$ were computed to attain the values of K and n .

RESULTS AND DISCUSSION

Melting behavior

The melting thermograms of pure PLA obtained by DSC after isothermal crystallization at various isother-

mal crystallization temperatures (T_c) are presented in Figure 1(A,B). For the samples that were isothermally crystallized at 85 and 90°C, a small crystallization exothermic peak was observed prior to the major melting endothermic peak in the heating scans. This small exothermic peak was an additional crystallization that occurred at a higher temperature during the DSC heating scan than the temperature at which the first crystallization occurred. As the T_c increased, the small exothermal peak gradually disappeared and a shoulder melting peak prior to the major melting peak appeared instead [Fig. 1(A,B)]. In the T_c range from 95 to 105°C, the transition from the additional crystallization (exothermal peak) to melting (endothermal peak) became evident. The blend that was isothermally crystallized at 105°C had a visible lower melting temperature peak followed by the major melting peak. After that, these two melting peaks gradually merged together and shifted to a lower temperature. The melting temperature of the blends increased as the T_c increased in the temperature range we evaluated [Fig. 1(B)]. Two groups of melting temperatures were observed (Fig. 2). One group of blends was isothermally crystallized from 85 to 105°C and the other from 110 to

125°C. In each group the melting temperature of the blends increased as the T_c increased, but there was a sharp drop at a T_c of 110°C. The additional crystallization had a slight effect on the melting temperature up to a T_c of 105°C, and the melting temperature increased slightly as the T_c increased. After 105°C two melting peaks were observed and they merged into one peak, which shifted toward a lower melting temperature; this merged melting peak temperature increased as the T_c increased. The transition from two peaks to one peak occurred in the T_c range of 105–115°C. Such a phenomenon was evident for blends of PLA with either starch [Fig. 3(A,B)] or talc [Fig. 3(C)].

The T_c also affected the fusion enthalpy of pure PLA and its blends with starch and talc. The fusion enthalpies of all the samples are shown in Table II. They increased almost linearly as the T_c increased for pure PLA and PLA/starch blends. This is because the additional crystallization increased as the T_c increased. However, the fusion enthalpies of PLA/talc (TalcPla1-99, Table II) changed only slightly and had no evident tendency. This is probably due to the high nucleation density caused by talc, which hindered crystal development.

Isothermal crystallization behavior

Typical crystallization isotherms, which were obtained by plotting the degree of crystallization $X(t)$ versus t , are shown in Figures 4 and 5 for pure PLA and its blends with starch and talc. The crystallization isotherm curves shifted along the time axis. At lower T_c temperatures, the curves shifted from right to left; at higher T_c , the curves shifted to the right. By plotting the T_c against the half-time of crystallization ($t_{1/2}$), defined as the time required to reach 50% of the final crystallinity, saddle shape curves for pure PLA and its blends with starch were obtained (Fig. 6). Absolute temperature units (K) was used for these plots according to the theory of isothermal crystallization kinetics. As indicated in theory, the undercooling was relatively high and crystal growth was the dominant factor determining the overall crystallization rate at low T_c . As the T_c increased, the undercooling was relatively low and nucleation was the dominant factor determining the overall crystallization rate. The minimum $t_{1/2}$ is 13.6 min at a T_c of 373 K (100°C) for PLA and 1.8–3.2 min at a T_c of around 378 K (105°C) for PLA/starch blends with various ratios. The crystallization rates of the blends containing starch were much faster than that of pure PLA [Fig. 6(A,B)] at all experimental temperatures (T_c), indicating that starch can increase the crystallization rate of PLA. Furthermore, as the starch content in the blend increased, the $t_{1/2}$ decreased slightly, indicating that the crystallization rate of PLA was slightly increased. Talc is one of the most effective nucleating agents. The $t_{1/2}$ for the blend

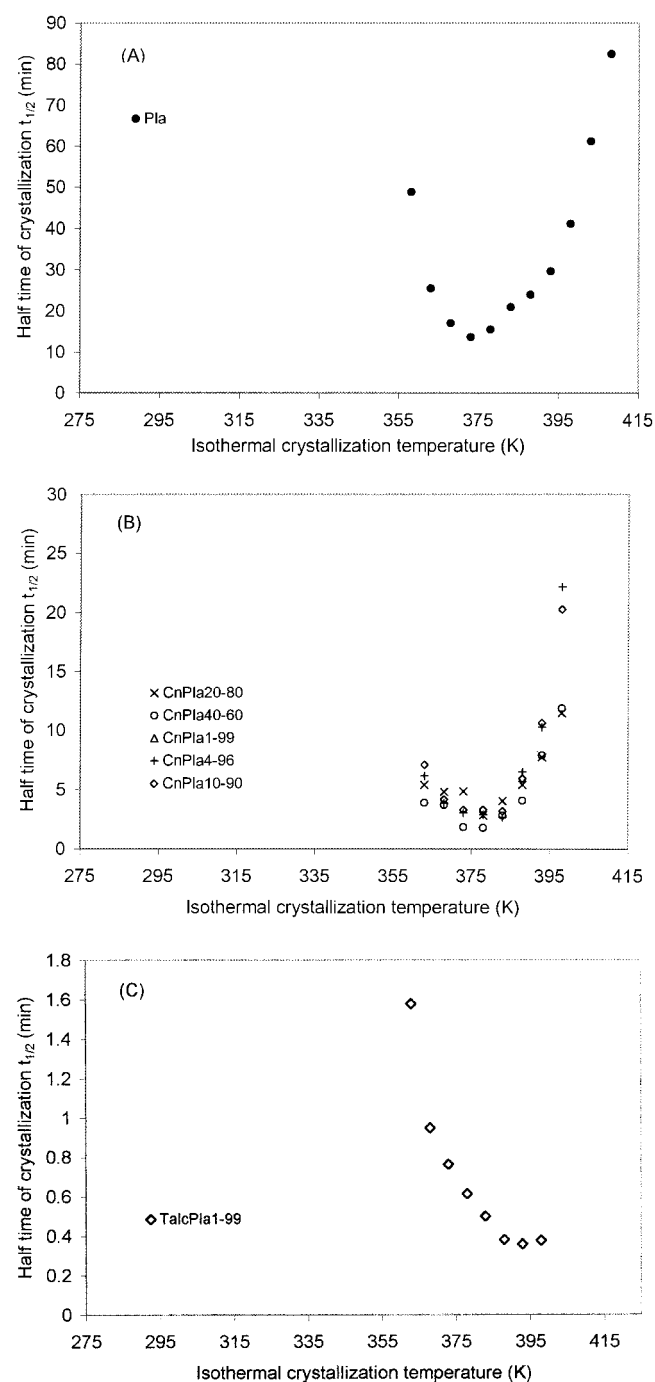


Figure 6 The half-time of crystallization ($t_{1/2}$) as a function of the isothermal crystallization temperature (T_c) for (A) PLA, (B) PLA/starch blends, and (C) PLA/talc blends.

of PLA/talc (TalcPla1-99) decreased as the T_c increased, and the $t_{1/2}$ for PLA at a T_c above 388 K (115°C) is 0.4 min [Fig. 6(C)]. At a T_c above 398 K (125°C) it was difficult to record or analyze the data because of the fast crystallization rate. This showed that talc is a stronger nucleating agent than starch in blends with PLA.

Figures 7 and 8 contain plots of $\ln[-\ln(1 - \alpha)]$ versus $\ln t$ according to eq. (2) for pure PLA and its

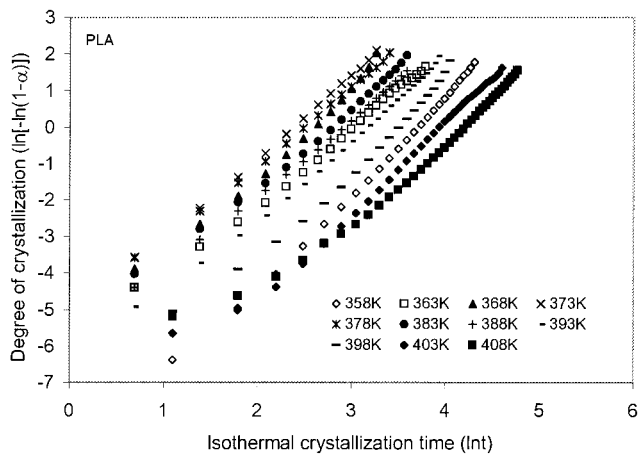


Figure 7 Plots of the degree of crystallization $\ln[-\ln(1-\alpha)]$ versus the crystallization time $\ln t$ for isothermal crystallization of pure PLA.

blends with starch and talc, respectively. The experimental data fit the Avrami equation very well for the early part of the transformation and became slightly nonlinear toward the end. This was more evident in

blends than in pure PLA. The crystallization process in PLA might not meet all prerequisites for using the Avrami equation and the calculation was also affected by the choice of ΔH_∞ . For example, the additional crystallization that occurred as discussed before would be a major factor in the equation. However, the Avrami method can still be used to roughly characterize the isothermal crystallization behavior of PLA and its blends with starch and talc. Table II lists the values of k and n at different crystallization temperatures for all samples obtained from linear fitting of the Avrami equation at early transformation.

The Avrami exponent n differs from sample to sample, and it also varies with T_c (Table II). The average n value in the T_c range tested was 2.19 for pure PLA; 1.78 for PLA/talc; and 2.27, 2.25, 2.31, 2.08, and 1.90 for starch/PLA at ratios of 1:99, 4:96, 20:80, and 40:60, respectively. As the starch content increased to 40%, the n value slightly decreased. The n value is affected by many factors, such as the nucleation density and restriction of crystalline formation due to filler concentration, which is not well understood in this study.

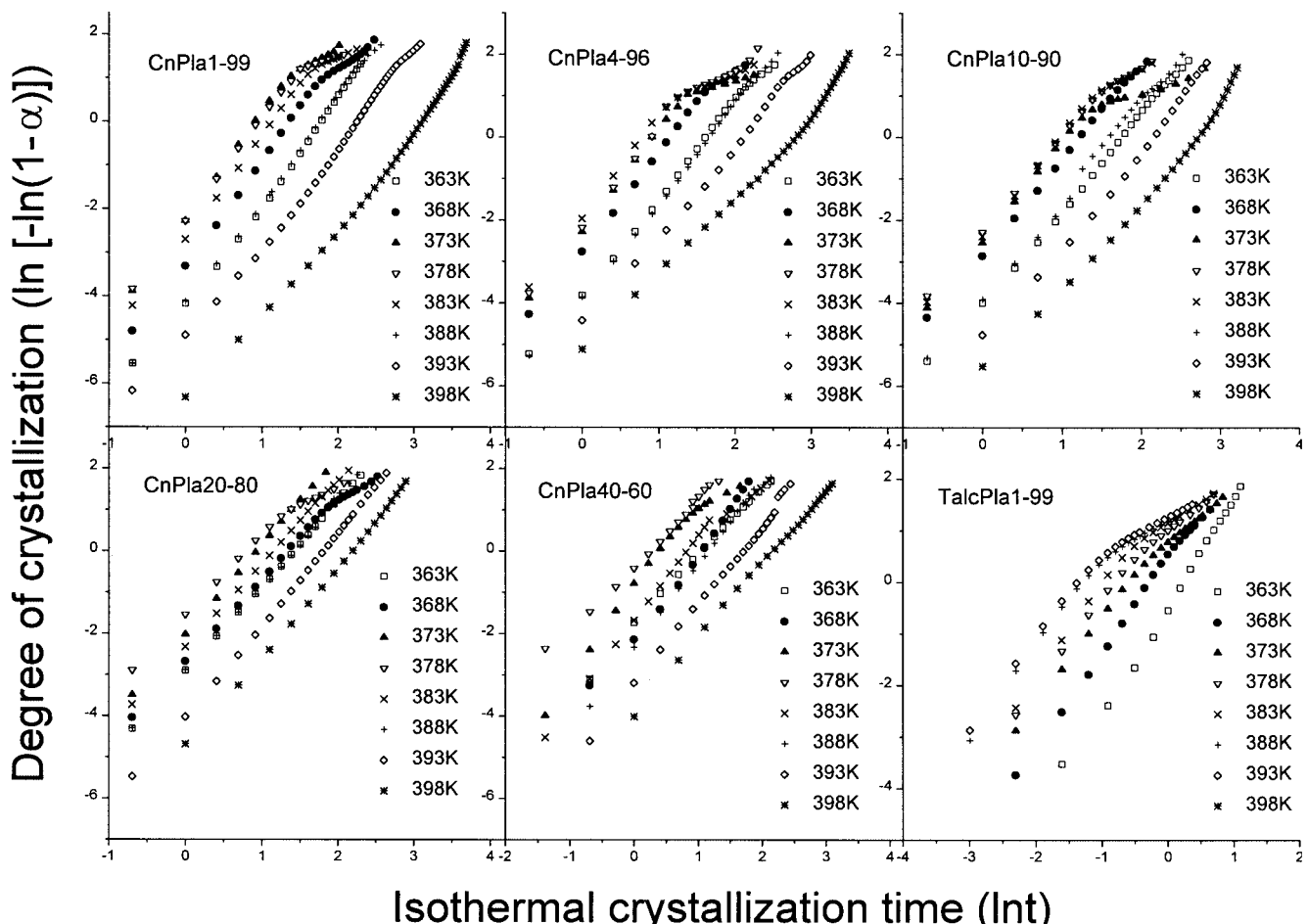


Figure 8 Plots of the degree of crystallization $\ln[-\ln(1-\alpha)]$ versus the crystallization time $\ln t$ for isothermal crystallization of PLA/starch blends and PLA/talc blends.

Both the rate of nucleation and the growth processes determined the rate constant k . As shown in Table II, at the same T_c , the k value for PLA/talc is the largest, the k values for all PLA/starch blends are in the middle, and the k value for pure PLA is the smallest. This further confirms that starch, although not as effective as talc, can be considered as a nucleating agent during crystallization of PLA. The k values first increased as the T_c increased and then decreased, similar to the tendency for $t_{1/2}$ (Fig. 6), but in the opposite direction.

CONCLUSION

The crystallization behavior of PLA/starch blends from the melt is mainly influenced by the composition and the crystallization temperatures. The starch in PLA/starch blends can effectively increase the crystallization rate of PLA, even at a content of 1%, but such an effect was less than that caused by talc. The crystallization rate increased slightly as the starch content in the blend increased. An additional crystallization of PLA was observed and increased as the crystallization temperature increased, which lowered the

melting point and increased the degree of crystallinity of PLA.

References

1. Ke, T.; Sun, X. S. *Cereal Chem* 2000, 77, 761.
2. Ke, T.; Sun, X. S. *J Appl Polym Sci* 2001, 81, 3069.
3. Ke, T.; Sun, X. S. *Trans ASAÉ* 2001, 44, 945.
4. Nijenhuis, A. J.; Grijpma, D. W.; Pennings, A. J. *J Polym Bull* 1991, 26, 71.
5. Kalb, B.; Pennings, A. J. *Polymer* 1980, 21, 607.
6. Cohn, D.; Younes, H.; Marom, G. *Polymer* 1987, 28, 2018.
7. Migliaresi, C.; de Lollis, A.; Fambri, L.; Cohn, D. *Clin Mater* 1991, 8, 111.
8. Kolstad, J. *J J Appl Polym Sci* 1996, 62, 1079.
9. Urbanovici, E.; Schneider, H. A.; Brizzolara, D.; Cantow, H. *J Therm Anal* 1996, 47, 931.
10. Kishore, K.; Vasanthakumari, R.; Pennings, A. J. *J Polym Sci Polym Phys Ed* 1984, 22, 537.
11. Vasanthakumari, R.; Pennings, A. J. *Polymer* 1983, 24, 175.
12. Tsuji, H.; Ikada, Y. *Polymer* 1995, 36, 2709.
13. Migliaresi, C.; Cohn, D.; de Lollis, A.; Fambri, L. *J Appl Polym Sci* 1991, 43, 83.
14. (a) Avrami, M. *J Chem Phys* 1939, 7, 1103; (b) Avrami, M. *J Chem Phys* 1940, 8, 212; (c) Avrami, M. *J Chem Phys* 1941, 9, 177.